Available online at www.sciencedirect.com
ScienceDirect
Catalysis Today 118 (2006) 360–365
CATALYSIS TODAY
www.elsevier.com/locate/cattod

Characterization and FT-IR study of nanostructured alumina-supported V-Mo-W-O catalysts

M.O. Guerrero-Pérez, M.C. Herrera, I. Malpartida, M.A. Larrubia, L.J. Alemany *

Departamento de Ingeniería Química, Universidad de Málaga, Campus de Teatinos s/n, E-29071 Málaga, Spain

Abstract

The effect of tungsten incorporation in the surface composition and its catalytic performance is evaluated for alumina supported Mo-V-O, Mo-W-O, V-W-O and Mo-V-W-O nanostructurated-oxide catalysts. The characterization results reveal that the surface of Mo-V-W-O catalysts is further different from the binary counterparts, due to the presence of stabilized and reduced structures dispersed on the support. Such species are not present in the Mo-V-O catalysts; indicative that tungsten acts as a structural–chemical promoter. The in situ FT-IR study of these catalysts under propane + oxygen atmosphere showed that Mo-V-W-O catalyst is able to thermally activate the propane oxotransformation and ODH-products are registered in the gas-phase whereas oxygenate-compounds are detected on the surface of catalysts.

Keywords: V-Mo-O; V-Mo-W-O; Nanoscaled oxides; Oxidation; Propane; Structure–activity relationship; In situ Raman; XRD; FTIR; XPS

1. Introduction

Most catalysts for selective oxidation to functionalized hydrocarbon molecules, possess vanadium as a key element [1–9]. Vanadium containing bimetallic-oxide catalysts are efficient for alkane-oxotransformation to olefins, oxygenates and nitriles [2–10]. Mo-V-O oxides are being investigated as catalysts for many oxidation reactions [11], especially for the dehydrogenation (ODH) of light saturated hydrocarbon, as propane [12–15], the ammoxidation to acrylonitrile [16–21] or the selective propane oxidation to acrylic acid [22–25]. The effect of the incorporation of Mo to V-containing catalysts results in a replace of the polyvanadate structure with less reactive V–O–Mo structure, leading to lower reducibility and oxidative dehydrogenation rates [13,14].

V-W (or Mo) catalysts supported on titania are commonly used for De-NO_x SCR by ammonia [26–29]. These bimetallic supported catalysts are known to have a wider SCR-temperature window activity than vanadium ones [30,31]. Also, tungsten was used as second component in Sb-V-O catalysts for propane ammoxidation and it was reported that the tungsten favours the selectivity towards acrylonitrile [32].

The bimetallic containing V system can be, apparently, tuned with a third component incorporation to catalyst formulation [10], as W or Mo. Multimetallic Mo-V-W-O bulk oxides appear to be promising as catalysts for selective oxidation processes [33–36] and this system is claimed as the most selective for the oxidation to acrylic acid from acrolein. At least two different Mo-V-W-O phases have been identified in bulk Mo-V-W-O catalysts [33]. It has been demonstrated that there is an improvement of the catalytic performance in the acrolein oxidation related to the formation of a $(MoVW)_5O_{14}$-type mixed oxide [34,35]. But some more structures have been identified in these catalysts; especially a $(MoVW)_2O_{5-x}$ structure that appears to be involved in the catalytic cycle [36].

It is the aim of present work to analyze the surface composition and catalytic behaviour of bimetallic systems (MoV, MoW and VW) and compare the results with those obtained with the MoVW sample in order to evaluate the possible synergism of the metallic-oxide species. Mo-V-W-O nanoscaled oxides have been stabilized to avoid the formation of clusters on alumina support, allowing a better insight of the nature of the active sites [37–38].

The overall reactivity is evaluated considering that the multioxide catalysts posses a superficial sensitivity to oxygen and also a certain capacity to activate hydrocarbons. This fact is determined by metallic electronic interactions, adsorption affinity and mobility of lattice oxygen.

---

* Corresponding author. Tel.: +34 952 13 1919; fax: +34 952 13 2000.
E-mail address: luijo@uma.es (L.J. Alemany).

0920-5861/$ – see front matter © 2006 Elsevier B.V. All rights reserved.
doi:10.1016/j.cattod.2006.07.012

2. Experimental

The synthesis of the catalysts was carried out by incipient wetness impregnation method in one step of the Al_2O_3 support (Alpha Aesar, 150 $m^2\,g^{-1}$); using ammonium metanavanadate (NH_4VO_3), ammonium molybdate tetrahydrated ($(NH_4)_2MoO_4{\cdot}4H_2O$) or ammonium metatungstate hydrated ($(NH_4)_6W_{12}O_{39}{\cdot}xH_2O$) as metals precursors using oxalic acid as complexing agent. The solution was kept at least for 12 h before impregnation to be sure that it was totally stabilized. Materials were dried during 12 h at 373 K (100 °C) in air and then calcined at 873 K (600 °C) during 2 h. Catalysts were prepared with a coverage of eight atoms for nm^2 of support. Mo/V, V/W and Mo/W atomic ratio values were fixed at 1 for all the samples.

Nitrogen adsorption isotherms were recorded (outgassed at 413 K for 2 h) on an automatic Micromeritics ASAP-2000 apparatus. X-ray diffraction patterns (XRD) were recorded on a Siemens D-501 diffractometer using Cu Kα radiation (operation value 40 kV and 22.5 mA) registered Bragg's angles between 10 and 70°. UV–vis spectroscopy in diffuse reflectance (UV–vis-RD) was recorded using a Jasco V-570 model spectrometer between the 200–800 nm of wavelength. Spectra are normalized according to Kubelka-Munk function.

Raman spectra were carried out with a single monochromatic Renishaw System 1000 equipped with a cooled CCD detector (−73 °C) and holographic super-Notch filter. The holographic Notch filter removes the elastic scattering while the Raman signal remains very high. The samples were excited with the 514 and 632.8 nm lines. Spectra were registered under dehydrated conditions (ca. 120 °C) in a hot stage (Linkam TS-1500) under dry air stream. Hydrated samples were obtained at room temperature after and under exposure to a stream of humid synthetic air.

Photoelectronic spectra (XPS) were acquired with a physical electronic 5700 spectrometer equipped with a hemispherical electron analyser and Mg Kα X-ray exciting source (1253.6 eV, 15 kV, 300 W). Binding energies (BE) were calculated using the C_{1s} peak at 284.9 eV. The accuracy of the BE values was ±0.2 eV. A strategy was established for the mathematical deconvolution and in all cases we adjust the signal, after background subtraction, to a mathematical response consistent of a distribution Gaussian–Lorenztian (80–20%, respectively) with an error χ^2 minimum; the contribution of each signal to the global one, expressed as relative percentage is the area under the curve and the maximum of the distribution are associated to the value of the bond energy.

FTIR spectra were recorded on a Nicolet Avatar 360. The coadsorption in situ reactivity runs were performed using pressed disks of the pure powders activated by outgassing at 773 K in the IR cell. Runs were performed in propane/oxygen (2/1) static atmosphere considering the thermally evolution registering simultaneously the surface response and the gas-phase spectra.

3. Results

Table 1
Equivalent composition (wt.%) and surface area (BET) of the supported catalysts

	V (wt.%)	Mo (wt.%)	W (wt.%)	A_{BET} ($m^2\,g^{-1}$)
Mo-V	3.63	6.99	–	114
Mo-W	–	7.37	12.70	116
V-W	3.72	–	13.78	113
Mo-V-W	2.50	4.69	9.15	129

The composition and A_{BET} of the catalysts are listed in the Table 1. The area values are quite similar for all the bimetallic samples (113–116 $m^2\,g^{-1}$) as expected since all of them posses the same coverage (superficial atomic density). It should be noted that the trimetallic sample (MoVW) presents a slight deviation (129 $m^2\,g^{-1}$) with respect the bimetallic counterpart. The difference regarding the support (~190 $m^2\,g^{-1}$) might correspond with the overall alumina dispersion capacity.

XRD patterns of catalysts are shown in Fig. 1. Weak features near 46 and 68° are detected in all samples and correspond to the alumina support (JCPDS file 37-1462). Two weak signals (low-signal/background ratio) near 23.6 and 34.1° appears in the XRD patterns of the bimetallic W containing samples (MoW and VW) and correspond to the most intense peaks of WO_3 (JCPDS file 83-0951). A feature near 38.2° is detected in all the samples. It is probably associated to different multimetallic segregate oxides. For the trimetallic catalyst, MoVW, no signals are further evidenced.

Fig. 2 shows the electronic profiles (UV–vis-DR) of the alumina-supported catalysts. While the alumina is almost transparent in the UV–vis whole region, the bimetallic catalysts which include vanadium in their formulation (VW and MoV), present a similar wavelength wideness with the maximum close to 350–370 nm and superimposed a shoulder to 260 nm; whereas the main absorption intensity for MoV decreases. For bimetallic Mo-containing catalysts the substitution of V for W produces a blue-shift of the absorption signal, and the FWHM of the signal becomes lower. In the 200–500 nm region the different absorptions are associated to charge transfer transitions ($O^{2-}\rightarrow M^{n+}$) [39] from the O_{2p} valence bands of the supported oxides to the V_{3d} (lowest energy compares with those of Mo and W levels), Mo_{4d} and W_{5d} orbital distanced to the bulk individual oxides. Only for MoV catalyst is detected some

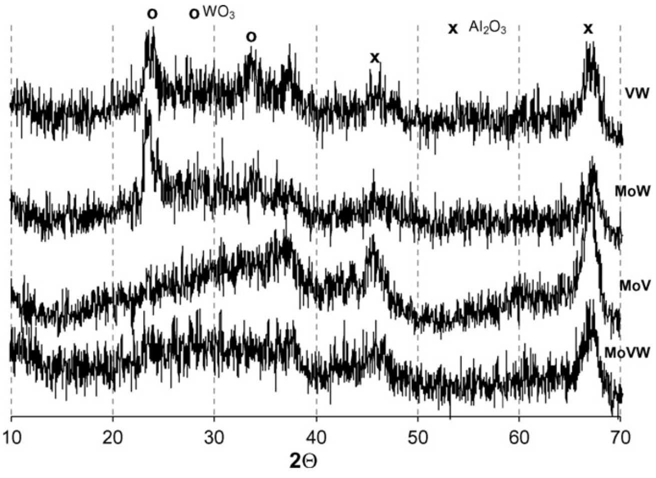

Fig. 1. XRD patterns of Mo-V-W-O/Al_2O_3 catalysts.

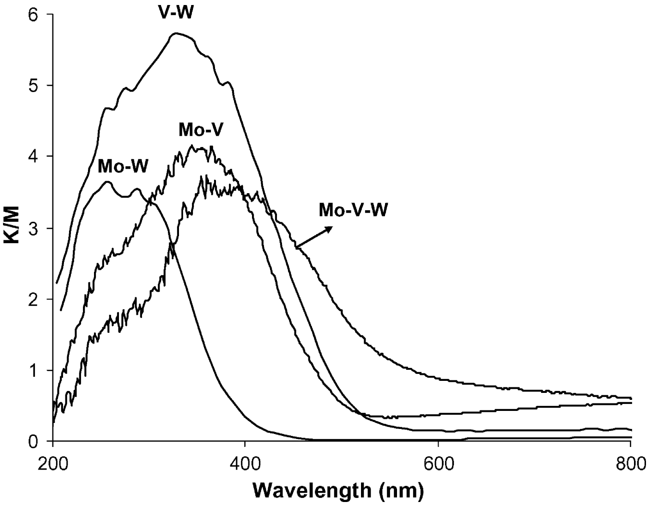

Fig. 2. UV–vis–NIR spectra of Mo-V-W-O/Al_2O_3 catalysts.

absorption in the visible region and is associated to d–d transitions of reduced centers.

The MoVW electronic profile is different from those obtained for the binary samples and the spectrum is not an intermediate situation between the Mo-containing catalysts spectra. A synergism between metallic centers is suggested: the maximum is shifted to higher wavelengths (390 nm) and the absorption intensity has decreased, also, an absorption in the whole visible region is observed. It should be considered the presence of quasi-free electrons or d–d transitions of the reduced metallic centers that are sensitive to outgassing and the visible radiation. This shows that when V, Mo and W are added to the alumina support, the metallic-oxide centres differ from those presented in the binary samples. An electronic interaction between oxide–surface species may occur through oxygen bridging of the polyhedral structure, facilitated by a lower equivalent overall coordination [39,40].

In Fig. 3 are shown the Raman spectra registered with the 514 nm exciting line. By using the line of 632.8 nm differences in the spectra of bimetallic catalysts were not observed; however the Raman profile is enhanced due to exciting line for MoVW sample. The spectrum of MoW sample show broad Raman bands near 800, 700 and 270 cm^{-1} typical of WO_3 polymorphic oxide [41], in agreement with the incipient XRD-signal observed. Probably incipient WO_3 nanocrystallites are detected in VW sample according to the Raman spectrum, which shows weak signals of this compound. A very weak, broad and asymmetric mode near 1000 cm^{-1} is detected in the Raman profile of the binary samples, and it is sensible to hydrating conditions. This broad feature could be correlated to M=O terminal stretching mode of surface-oxide species [26,41,42]. No Raman bands corresponding to V_2O_5 or MoO_3 segregate oxides were detected for VMo sample. The Raman spectrum shows a broad signal close at 1000 cm^{-1} and superimposed a weak-shoulder at 1024 cm^{-1}; sensible under hydrating conditions, assigned M=O stretching modes [42] of dispersed V-Mo-O_x species, respectively. Besides a broad signal centered at 860 cm^{-1} is also registered in the Raman profile, that it might be associated to the polymeric Mo-O-V alumina bidimensional superficial species.

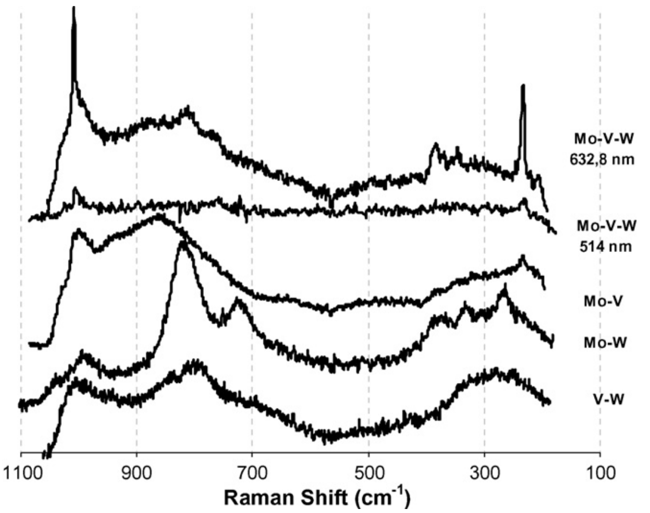

Fig. 3. Raman spectra of Mo-V-W-O/Al_2O_3 catalysts excited with the 514 nm line and spectrum of Mo-V-W sample excited with the 632.8 nm line.

The Raman spectrum using the exciting line of 514 nm of MoVW catalyst is further different. It could be detected two very weak signals near 1007 and 230 cm^{-1}. These modes are enhanced when the 632.8 nm exciting line is used; and also weak signals near 770, 370 and 330 cm^{-1} are evidenced. These enhanced bands have been previously detected for higher metal loading, above monolayer, for alumina supported Mo-V catalysts by Bañares et al. [13] and by Iglesia and co-workers [14,43] when the catalysts have undergone an activation process or after reaction. The modes at 1007, 230 and 770 cm^{-1} appear to arise from common V-Mo oxo-structure containing V–O–Mo bonds, but a definitive assignment has not been performed yet [14]. Some features near 860 and 800 cm^{-1} can be appreciated in Raman spectrum of MoVW sample excited with the 632.8 nm line. These bands have been attributed to the presence of partially reduced Mo–V–O phases for bimetallic Mo and V containing catalysts, detected in bulk systems or when the metal loading excess the dispersion capacity of the support [13,44–46]; these bands are not detected over multimetallic supported fresh-catalysts with an overall loading close to a monolayer alumina surface coverage. The tungsten incorporation could induce a rearrangement of the polyhedral reduced metallic centers by electronic interaction, permitting a chemical stabilization of centers, even when the catalyst is calcined in air at higher temperatures. The loss of Raman signal might be associated to the scattering effect by the coupling of the exciting laser wavelength with an increasing absorption by the reduced centers density population. This effect is associated to a rearrangement of surface metallic with a more homogeneous coordination stabilized by tungsten incorporation.

Table 2 summarizes the XPS data. Mo^{6+} and Mo^{5+} surface species led to two unresolved bands close to 235.0 and 232.3 eV in agreement with the results obtained by Mestl et al. with bulk Mo-V-W samples [33]. Mo^{4+} species were detected as a separate contribution close to 230.9 eV. Curve fitting was conducted in order to determine the relative contributions of

Table 2
Binding energies (eV) and relative contribution of signals (%) for the supported catalysts

	V_{2p}	Mo_{3d}	W_{4f}
Mo-V	517.4 (73%) 516.1 (27%)	235.0–232.3 (91%) 234.0–230.9 (9%)	–
Mo-W	–	235.0–232.3	37.7–35.7
V-W	517.0 (36%) 516.1 (64%)	–	37.7–35.7
Mo-V-W	517.1 (32%) 515.9 (68%)	235.1–232.4 (91%) 233.8–230.7 (9%)	37.5–35.5

Mo^{6+}/Mo^{5+} and Mo^{4+} species. The spin-orbit splitting between the $Mo_{3d5/2}$ and $Mo_{3d3/2}$ signals was fixed to 3.1 eV and the intensity ratio was set to 0.67. The relative population of Mo^{6+}–Mo^{5+} and Mo^{4+} resulted 90/10(%), respectively, for the V-containing samples. For the V-free sample, no Mo^{4+} associated signals were detected. Only one signal of W^{6+} is detected for all the samples (Table 2), indicative that W is not reduced. The V_{2p} signal is contribution of two components. The one at higher BE (above 517.0) is assigned to V^{5+} species and the second at lower binding energy is associated to V^{4+} [33]. Samples containing tungsten (VW and MoVW) present the majority of vanadium population reduced as V^{4+} whereas for sample MoV the 73% of them appear to be oxidized as V^{5+}. So, it appears that tungsten induces vanadium species to remain reduced as V^{4+}. These results are in agreement with those reported in literature for bulk Mo-V-W mixed oxides [33]. It should be notice that BE values seem to shift depending the metal incorporated to the formulation, probably by the chemical environment modification induced by the presence of a third component.

Fig. 4 shows the in situ oxotransformation ($C_2H_8/O_2 = 40/20$ relative pressure in torrs) after a thermal activation in vacuum (RT to 400 °C) carried out by FTIR (i.e. molecular approaching considering the surface and the homogeneous phase rounded the pellets inside the IR-cell). The experiment was performed over MoV (A and B, respectively) and MoVW (C and D).

Fig. 4A shows that there are not surface species adsorbed on the surface of MoV catalyst. Simultaneously, in the spectrum of the gas phase (the initial mixture of gas contribution was substrated), species corresponding to a partial overoxidation were not detected.

A suggestive change was registered with the W-containing catalyst. Fig. 4C shows broad features between 1350 and 1560 cm^{-1} associated to acetate and enolate species [47]. To higher wavenumbers a band close to 1680 cm^{-1} can be appreciated, related to acetone [48] and/or carboxilates [49] as superficial retained species that appears at 100 °C. These features (1370, 1460, 1560 and 1630 cm^{-1}) are in agreement with the acrolein adsorbed spectra reported by Davydov [50]. In the spectra of the gas-phase are detected the modes associated to oxidation products as CO (2172 and 2123 cm^{-1}), CO_2 (2359, 2338 and 667 cm^{-1}) and ODH-derivate: mainly propylene (990 cm^{-1}) detected at the highest temperature (400 °C, Fig. 4D).

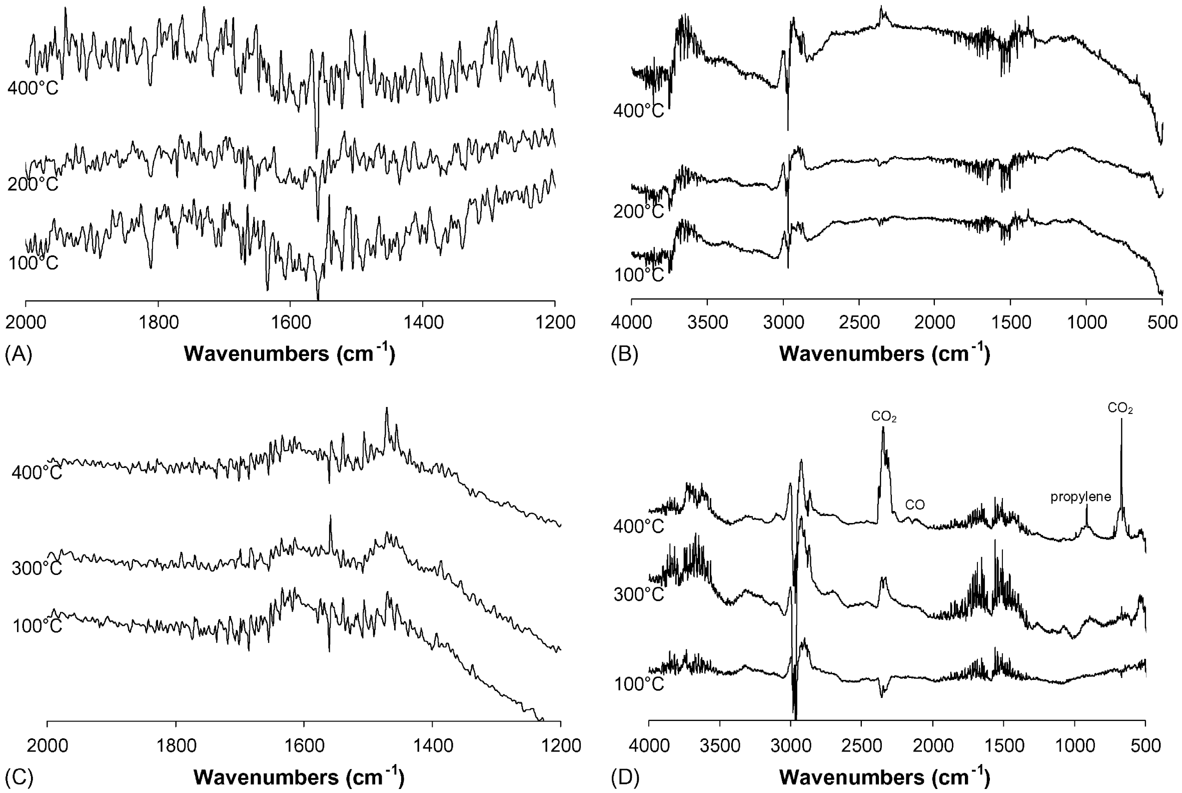

Fig. 4. In situ FTIR spectra of Mo-V and Mo-V-W catalysts under propane oxidation environment (propane and oxygen). (A) Mo-V and (C) Mo-V-W catalysts (activated catalysts and gas phase spectra have been subtracted). (B) Mo-V and (D) Mo-V-W gas phase (gas phase spectrum at ambient temperature has been subtracted).

4. Discussion

The preparative protocol (a single step) of the catalysts, with loading close to the theoretical dispersion capacity of alumina, facilities the mixed spreaded structures formation between Mo, V, and W [51,52] hindering the phases segregation. Only tungsten appears as incipient WO_3 nanocrystals according to Raman spectra (Fig. 3) in the sample MoW; in accordance with Wachs results that showed than the amount of W atoms on one monolayer of alumina is close to 4.0 [53], value close to that loaded in this sample. Mo-V-W alumina supported system has shown a different overall behaviour quite different that the corresponding binary counterparts. The W presence by incorporation to MoV catalyst produces a partially reduced and stabilized superficial structure. These structures are detected by the electronic spectra (UV–vis-DR, Fig. 2), whose maximum is shifted to 390 nm, the relative intensity decreases and the profile is extended to the visible region. Also a modification is observed in the Raman profile since two outstanding modes sensitive with the line exciting wavelength are detected. In addition, the XPS data also indicate a change in the reduced population species ratio (Table 2), V is as V^{5+} in Mo-V sample whereas the majority of V is partially reduced in the MoVW sample. The minor modification of the BE values is determined primarily by interaction between the metallic superficial centers.

It is interesting to note that the amount of Mo and V in the binary sample is higher (50% of theoretical surface coverage of each one and as the relative atomic percentage) than in the Mo-V-W sample; whose relative nominal content is about 0.33 of the total coverage in order to maintenance the relative metal–metal atomic ratio. So, we could expect that is easier that Mo and V interact to form mixed structures in the binary sample, but the characterization results clearly show that Mo-V-O reduced phases are detected in the Mo-V-W sample. Vanadium spectral features for the ternary alumina supported system nicely indicate that the main interaction is between the co-supported oxide structures while the alumina interaction is certainly weaker. The above observations underline the existence of a mutual electronic interaction that may operate via oxygen bridging rearrangement conditioned by the mixed and stabilized metallic spread structure.

In situ catalytic runs, considering $C_2H_8/O_2 = 2/1$, showed that alumina is not controlling the reaction pathway. The W incorporation, apparently, induces that the superficial amount of propane retained is higher than for bimetallic catalyst. Besides MoVW catalyst can activate the propane molecule under relatively mild conditions. The presence of weak-modes associated to acetone and acetate species, major over-oxidation precursors, is probably consequence of a residual Bronsted acidity. The W incorporated to MoV catalyst produces an improvement of propane-ODH and releases in the gas phase of propylene. The propylene partial retained undergoes an ulterior partial oxidation by interaction with the nucleophilic lattice oxygen to produce acrolein that might be latter release. The selectivity to propylene must be achieved by interaction with less-nucleophilic superficial species than surface oxygen ions. This fact involves to the superficial oxygen species with an appropriate site to transform the propane molecule to propylene, facilitating the release into gas-phase. However to transform the propane molecule into oxygenates (acrolein) requires a modification of the electron transfer through the catalyst surface oxygen mobility: involving both a reactant-sites geometry as a superficial defects equilibrium that could be established by the presence of a third component as tungsten.

Surface vanadium and molybdenum are the active surface sites in propane ODH [13–15,24], and it is reported that do not present appropriate results in the production of oxygenates [24,54]. In V-Mo-O (bulk or quasi-bulk systems) vanadium population is essentially as V^{5+}, but the incorporation of Te or Nb induces the formation of V^{4+} species improving the selectivity to oxygenates [24,48]. Also, it is reported that when Sb is added to V-based catalysts, V^{4+} is stabilized by formation of $VSbO_4$ phase, improving acrylonitrile selectivity [38,55,56]. These results are in line with those obtained in present paper. The differences founded in the characterization of Mo-V and Mo-V-W supported samples showed how the population of reduced vanadium species is higher when tungsten is present. The differences in the reactivity of both samples is underlined by the in situ-FTIR experiments that showed how propylene and oxygenates are detected on the gas-cell and the surface of catalysts under reaction environment whereas these are not registered on the surface of Mo-V sample. So, vanadium reduced and stabilized in the superficial species are involved in the selective oxotransformations. Mo-V-W bulk systems are known to be active as partial oxidation catalysts, especially for the oxidation of acrolein to acrylic acid [33–36], involving vanadium reduced centers that were improved by thermal treatment, and the reactivity is related mainly to the oxygen mobility on the surface.

5. Conclusion

The results presented in this contribution clearly show how the incorporation of W to Mo-V catalysts leads to the stabilization of reduced Mo-V-O superficial structures enhancing the selectivity to propylene and oxygenates. The structure provides accessible active centers that improve ion mobility to the surface of catalyst. So, the addition of W leads to significant changes in the surface properties which affect both, catalyst activity and selectivity in the oxotransformation of propane. It can be tentatively assumed that a change in the superficial nanoscale rearrangement of multioxide centers (caused by the structural and chemical character of tungsten) is the reason for the changes observed in the in situ catalytic runs.

Acknowledgements

MOGP acknowledges the Ministry of Education and Science for a ‘‘Juan de la Cierva’’ post-Doctoral position. IM thanks the Junta de Andalucía for a FPDI fellowship. The authors thank Dr. M.A. Bañares (Institute of Catalysis and Petroleumchemistry, Madrid, Spain), and Dr. C. Resini (Università di Genova, Italy), for their help with Raman and UV–vis spectroscopies, respectively.

References

[1] R.K. Grasselli, Catal. Today 49 (1999) 141.
[2] T. Blasco, J.M. López-Nieto, Appl. Catal. A 157 (1997) 117.
[3] H. Jiang, W. Lu, H. Wan, J. Mol. Catal. A 208 (2004) 213.
[4] K. Oshihara, T. Hisano, W. Ueda, Top. Catal. 15 (2001) 153.
[5] M.A. Bañares, Catal. Today 51 (1999) 319.
[6] V.V. Guliants, Catal. Today 51 (1999) 255.
[7] E.A. Mamedow, V. Cortés Corberán, Appl. Catal. A 127 (1995) 1.
[8] I.E. Wachs, Catal. Today 100 (2005) 79.
[9] A. Christodoulakis, M. Machli, A.A. Lemonidou, S. Boghosian, J. Catal. 222 (2004) 293.
[10] G. Deo, I.E. Wachs, J. Catal. 146 (1994) 335.
[11] A. Bielanski, M. Najbar, Appl. Catal. A 157 (1997) 223.
[12] J.D. Pless, B.B. Bardin, H.S. Kim, D. Ko, M.T. Smith, R.R. Hammond, P.C. Stair, K.R. Poeppelmeier, J. Catal. 223 (2004) 419.
[13] M.A. Bañares, S.J. Khatib, Catal. Today 96 (2004) 251.
[14] S. Yang, E. Iglesia, A.T. Bell, J. Phys. Chem. B 109 (2005) 8987.
[15] Z. Zhao, X. Gao, I.E. Wachs, J. Phys. Chem. B 107 (2003) 6333.
[16] J.M. Millet, H. Roussel, A. Pigamo, J.L. Dubois, J.C. Jumas, Appl. Catal. 232 (2002) 77.
[17] M. Vaarkamp, T. Ushikubo, Appl. Catal. A: Gen. 174 (1998) 99.
[18] H. Tsuji, Y. Koyasu, J. Am. Chem. Soc. 124 (2002) 5608.
[19] M.O. Guerrero-Pérez, J.N. Al-Saeedi, V.V. Guliants, M.A. Bañares, Appl. Catal. A 260 (2004) 93.
[20] M. Baca, J.-M.M. Mollet, Appl. Catal. A 279 (2005) 67.
[21] H. Watanabe, Y. Koyasu, Appl. Catal. A 194–195 (2000) 479.
[22] V.V. Guliants, R. Bhandari, J.N. Al-Saeedi, V.K. Vasudevan, R. Soman, O. Guerrero-Pérez, M.A. Bañares, Appl. Catal. A 274 (2004) 123.
[23] J.N. Al-Saeedi, V.V. Guliants, M.O. Guerrero-Pérez, M.A. Bañares, J. Catal 215 (2003) 108.
[24] W. Ueda, D. Vitry, T. Katou, Catal. Today 96 (2004) 235.
[25] P. Botella, E. García-González, A. Dejoz, J.M. López Nieto, M.I. Vázquez, J. González-Calbet, J. Catal. 225 (2004) 428.
[26] L.J. Alemay, L. Lietti, N. Ferlazzo, P. Forzatti, G. Busca, E. Giamello, F. Bregani, J. Catal. 155 (1995) 117.
[27] M. Najbar, J. Camra, A. Bialas, A. Weselucha-Birczynska, B. Borzecka-Prokiop, L. Delevoye, J. Klinowski, Phys. Chem. Chem. Phys. 1 (1999) 4645.
[28] M. Najbar, E. Broclawik, A. Gora, J. Camra, A. Bialas, A. Weselucha-Birczynska, Chem. Phys. Lett. 325 (2000) 330.
[29] P. Kornelak, F. Mizukami, A. Weselucha-Birczynska, L. Proniewicz, G. Djega-Mariadassou, A. Bialas, M. Najbar, Catal. Today 90 (2004) 103.
[30] P. Forzatti, L. Lietti, HCR Compr. Rev. 3 (1996) 33.
[31] G. Busca, L. Lietti, G. Ramis, F. Berti, Appl. Catal. B 18 (1998) 1.
[32] J. Nilsson, A.R. Landa-Canovas, S. Hansen, A. Anderson, J. Catal. 186 (1999) 442.
[33] G. Mestl, Ch. Linsmeier, R. Gottschall, M. Dieterle, J. Find, D. Herein, J. Jäger, Y. Uchida, R. Schlögl, J. Mol. Catal. A 162 (2000) 463.
[34] M. Dieterle, G. Mestl, J. Jäger, Y. Uchida, H. Hibst, R. Schlögl, J. Mol. Catal. A 174 (2001) 169.
[35] O. Ovsitser, Y. Uchida, G. Mestl, G. Weinberg, A. Blume, J. Jäger, M. Dieterle, H. Hibst, R. Schlögl, J. Mol. Catal. A 185 (2002) 291.
[36] T. Uchida, G. Mestl, O. Ovsitser, J. Jäger, A. Blume, R. Schlögl, J. Mol. Catal. A: Chem. 187 (2002) 247.
[37] M.A. Bañares, Catal. Today 100 (2005) 71.
[38] M.O. Guerrero-Pérez, M.A. Bañares, Chem. Commun. (2002) 1292.
[39] M.A. Larrubia, G. Busca, Mater. Chem. Phys. 72 (2001) 337.
[40] M.A. Bañares, M.V. Martínez-Huerta, X. Gao, J.L.G. Fierro, I.E. Wachs, Catal. Today 61 (2000) 295.
[41] D.S. Kim, M. Ostromecki, I.E. Wachs, J. Mol. Catal. A 106 (1996) 93.
[42] M.A. Bañares, I.E. Wachs, J. Raman Spectrosc. 33 (2002) 259.
[43] H. Dai, A.T. Bell, E. Iglesia, J. Catal. 221 (2004) 491.
[44] G. Mestl, J. Raman Spectrosc. 33 (2002) 333.
[45] M. Dieterle, G. Weinberg, G. Mestl, Phys. Chem. Chem. Phys. 4 (2002) 812.
[46] M. Dieterle, G. Mestl, Phys. Chem. Chem. Phys. 4 (2002) 822.
[47] V. Ermini, E. Finocchio, S. Sechi, G. Busca, S. Rossini, Appl. Catal. A 198 (2000) 67.
[48] P. Concepción, P. Botella, J.M. López Nieto, Appl. Catal. A 278 (2004) 45.
[49] M. Baldi, F. Milella, G. Ramis, V. Sánchez Escribano, G. Busca, Appl. Catal. A 166 (1998) 75.
[50] A.A. Davydov, Infrared spectroscopy of adsorbed species on the surface of transition metal oxides. in: C.H. Rochester (Ed.), John Wiley & Sons.
[51] M.C. Herrera-Delgado, Ph.D. Dissertation, Universidad de Málaga, Spain (2004).
[52] M.O. Guerrero-Pérez, M.C. Herrera-Delgado, M.A. Larrubia, L.J. Alemany, Europacat VII, Sofia, Bulgaria, 2005.
[53] I.E. Wachs, Catal. Today 27 (1996) 437.
[54] T. Katou, D. Vitry, W. Ueda, Catal. Today 91–92 (2004) 237.
[55] M.O. Guerrero-Pérez, J.L.G. Fierro, M.A. Vicente, M.A. Bañares, J. Catal. 206 (2002) 339.
[56] M.O. Guerrero-Pérez, M.A. Bañares, Catal. Today 96 (2004) 265.